

Stainless Steel Hollow Sphere Foams- Fabrication, Carburization, and Properties

J. L. Clark, K. M. Hurysz, K. J. Lee, J. K. Cochran, T. H. Sanders, Jr.

School of Materials Science and Engineering
Georgia Institute of Technology
Atlanta, GA, 30332-0245, USA

Abstract

Lightweight stainless steel foams approaching 10% theoretical density are being fabricated via direct reduction. These foams are formed using a coaxial nozzle process that generates hollow ceramic spheres at high rates from an acetone-based slurry. The $\text{Fe}_2\text{O}_3/\text{Cr}_2\text{O}_3$ hollow spheres are reduced in a hydrogen/argon atmosphere at high temperature resulting in individual hollow metal spheres. Using more viscous slurry of similar composition, the spheres are bonded at points of contact into a quasi-closed cell structure and further heat treated to reduce the bond phase. The result is a Fe-12Cr alloy hollow sphere foam with a density on the order of 1 g/cc. Addition of carbon and further heat treatments allow the control of strength and ductility through microstructure. Mechanical testing is being conducted to determine attainable properties that can be compared to existing foam models.

1 Introduction

Structural foams offer a variety of properties that make their development important to many high technology industries such as automotive and aerospace. Foams can offer a lightweight means of stiffening a structural member, increasing energy absorption, dampening sound, or dissipating heat. Hollow sphere metal foams formed using the coaxial nozzle process^{1,2} possess a unique blend of properties and characteristics that suit them for these purposes. The research presented here focuses on the processing of hollow sphere stainless steel foams and their mechanical properties. Specifically, issues of scaling up to large bulk foams and comparison of experimental mechanical properties to predicted values are addressed.

Early processing of stainless steel hollow sphere structures used monolithic oxide foams that were directly reduced in hydrogen. Oxide shells generated from the coaxial nozzle process were initially fired in air to sinter the shells and allow handling with minimal damage. Once sintered, the spheres were packed together in a castable form using an aqueous bond slurry of similar composition. The bond slurry served to bind the spheres at points of contact and allow handling of the cast ceramic foams. Typical composition of the bond slurry consisted of a 75 wt.% solids loading of $\text{Fe}_2\text{O}_3/\text{Cr}_2\text{O}_3$ in the appropriate proportions as well as polymer additives to serve as binders and dispersants. Once dried, these monolithic oxide foams were heat treated in a hydrogen/argon atmosphere at 1400 °C. At this temperature, the mixture of Fe_2O_3 and Cr_2O_3 is converted to the alloy. However, direct heating to this temperature resulted in the melting of an intermediate phase, possibly FeO or a solid solution thereof. Consequently, a preheat to 1000 °C, where Fe_2O_3 would be mostly reduced, was added to eliminate melting of the intermediaries. Subsequent heating to 1400 °C allowed reduction of Cr_2O_3 and additional sintering of the metallic

material. Processing of small pieces of foam showed that wall porosity of less than 2% was obtainable with foam densities ranging from 0.7 to 1.6 g/cc.

Ideally, the end result of the reduction would be a well-sintered hollow sphere metal foam. However, significant dimensional instability was encountered during reduction processing that led to severe spalling and cracking of the foam structure. Oxygen loss combined with densification in the ceramic state produced approximately 60% volume shrinkage. The foam could not accommodate this severe dimensional change. Dilatometer tests were conducted to explore the degree of expansion and contraction occurring during reduction and to determine how to circumvent their deleterious effects.

Powders of Fe_2O_3 , Cr_2O_3 , Fe_3O_4 , and $88\text{Fe}_2\text{O}_3\text{-}12\text{Cr}_2\text{O}_3$ were pressed into pellets of approximately 6 mm thickness and 4 mm diameter. The samples were heated in the dilatometer to 1450 °C at 2 °C/min. Atmospheres of 4% H_2 in argon, pure argon, and air were investigated. Figure 1 shows the results of the dilatometry tests.

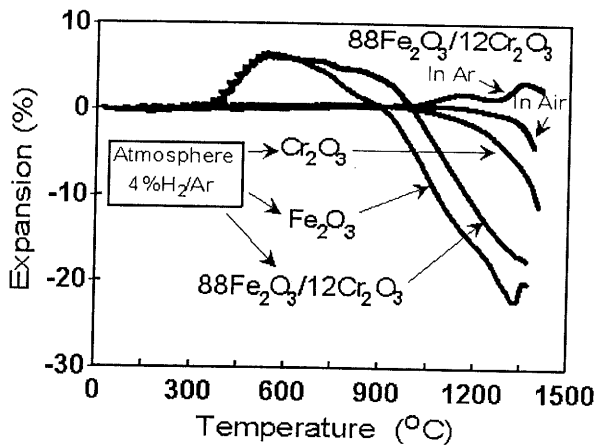


Fig. 1: Dilatometric traces for various oxide compositions in air, argon, and hydrogen/argon atmospheres.

The dilatometry profiles for Fe_2O_3 and $88\text{Fe}_2\text{O}_3\text{-}12\text{Cr}_2\text{O}_3$ clearly show significant expansion with a maximum in the range of 400 - 600 °C. This is well below the temperature at which the foam is reduced to metal and, consequently, the brittle ceramic body cannot survive the extensive expansion. This dilatometric data is further supported by literature on direct reduced iron and the structural changes that occur during stepwise reduction of Fe_2O_3 to Fe_3O_4 and FeO before final conversion to metallic iron. More specifically, it is the arrangement of the oxygen atoms in the lattice that results in the nearly 25 vol.% expansion observed. As the oxide is converted from hematite to magnetite, oxygen atoms arranged in a close-packed hexagonal structure reorient to form the face-centered cubic structure seen in magnetite and wustite. This serves to open up the structure and increase the tendency of the oxide body to reduce.³ While this was advantageous for reducing iron ore for raw materials, the volume expansion does not suit foam processing.

Now, net shape foams are being formed with little dimensional change in the bonding cycle. A one step thermal treatment in atmosphere reduces iron/chromium oxide powder shells, densifies the shell wall to near theoretical density, and prevents diffusion bonding of the spheres during reduction. The loose, dense wall spheres serve as the raw material for net shape foams. With this loose sphere processing technique, sphere wall defects are dramatically reduced as compared to multiple step firing. Densification is faster and more complete because individual spheres are free

to shrink to the center of mass. Bonding pre-fired, dimensionally stable spheres results in little shrinkage in the final thermal treatment that sinters the bond phase. This makes possible the forming of complex geometry sandwich panel structures by casting loose sphere mixes between curved face sheets.

Once suitable foams were processed, mechanical property data were collected. Compressive stress-strain behavior was used to evaluate the structural effect of the monolithic oxide foam reduction process as compared to the loose sphere reduction process. Additionally, the Fe/Cr alloy foams were characterized before and after carburization and heat treatment. Both solution carburization and gas carburization were used to diffuse carbon into the alloy bulk. As more compression data are collected, the extent to which hollow sphere foam properties follow the foam prediction models of Gibson and Ashby will be investigated.⁴

The structure described by Gibson and Ashby does not reflect the true structure of hollow sphere foams. Their model is based on cubical cells stacked in a space-filling configuration. The hollow sphere construction does not allow for a space-filling configuration and, consequently, generates both open and closed porosity.⁴ For this reason the structure is termed 'quasi-closed cell' and the properties are thus expected to fall between the open/closed cell predictions of Gibson and Ashby. Many metal foams available are of the open cell nature and, due to their processing, possess anisotropic properties below predicted values. For this reason, a quasi-closed cell foam with isotropic properties shows great potential.

2 Processing Results

2.1 Oxide Sphere Formation

Hollow oxide spheres were produced by passing an acetone-based slurry through the outer annulus of a coaxial nozzle. This produces a hollow cylinder of slurry. An inner-jet of an inert gas such as nitrogen is injected into the hollow cylinder resulting in instability. This causes the walls to pinch off and create hollow slurry spheres. As the spheres fall through a heated air updraft, the acetone evaporates from the sphere walls leaving an oxide shell bonded by polymer additives. The shells can then be further processed.

Slurry compositions consisted of acetone, Fe₂O₃ powder with a average particle size of 3 to 6 μm, Cr₂O₃ powder with a average particle size of approximately 2 μm, and polymethyl methacrylate binder/dispersant. Typically, a 46 vol.% solids loading was used with a 3% dwb addition of the binder/dispersant. After thorough mixing, a viscosity of approximately 50 cP was obtained. The slurry was then fed to the coaxial nozzle at a rate of approximately 20 mL per minute. Slurry feed rate and inner jet flow rate were adjusted to produce the most desirable sustained sphere production. Sphere formation rates of 5000-6000 spheres per minute were typical and monosized (± 4%) 2 to 3 mm diameter spheres resulted. Control of variables such as viscosity, slurry feed rate, and inner jet flow rate allows production of spheres with various sizes and wall thickness. The end result is the ability to control final foam density.

2.1 Fe₃O₄ Processed Foams

Further study of the dilatometric data mentioned previously revealed that, upon reduction in hydrogen, magnetite does not undergo the expansion seen in hematite. Dilatometer traces for magnetite and hematite reduced in hydrogen can be found in Figure 2. This data corresponds with the literature on the subject.³ Since there is no rearrangement of oxygen atoms in the conversion to FeO, expansion is significantly less and dimensional instability during processing is minimized. As suggested by its name, magnetite exhibits magnetic behavior. This precludes its use in a slurry that is suitable for the coaxial nozzle process. It is difficult to disperse the powder in acetone while maintaining a sufficiently high solids loading. As an alternative, attempts were made to convert

fired hematite foams to magnetite using a vacuum heat treatment. Based on the data of Darken and Gurry, it was determined that firing the hematite to high temperatures in low pO_2 would convert the hematite to magnetite.⁵⁻⁷ The magnetite could then be reduced by hydrogen firing.

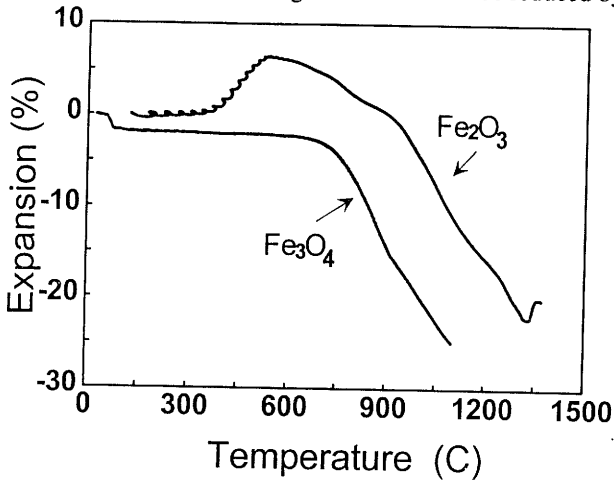


Fig. 2: Dilatometric traces for hematite and magnetite in hydrogen/argon atmospheres.

Using a vacuum furnace with graphite elements capable of 1350 °C at 10^{-5} torr, the hematite foams were successfully converted to magnetite. It is not entirely clear as to why this conversion process did not result in damage like the hydrogen reduction. It would seem that the much higher temperature at which the conversion occurred or a conversion mechanism unlike that in hydrogen reduction are responsible. Nonetheless, the magnetite foams were successfully reduced to metallic foams. Upon metallographic inspection of these metallic foams it was observed that there was significant porosity present. It was assumed that the porosity remained from the conversion process during which the structure, as suggested previously, opened up to accommodate oxygen transport. This additional porosity in the sphere walls serves only to degrade mechanical properties. Another solution was needed.

2.2 Loose Sphere Processing

The final processing approach returned to earlier work on the reduction of oxide hollow spheres. Individual hematite hollow spheres were reduced without the damage experienced in the bulk foams. The isotropic nature of the sphere allows accommodation of the expansion and contraction during reduction as opposed to bulk foams, where point contact bonds prevent uniform expansion. In order to process loose spheres in bulk without allowing premature diffusion bonding, green oxide spheres were dispersed throughout fired alumina hollow spheres. This bed of alumina spheres prevents diffusion bonding between the metallic spheres while allowing hydrogen to flow in and water vapor to flow out. Once reduced, the metallic spheres were magnetically separated from the alumina spheres and cast into foams.

The casting process was similar to that previously mentioned. Bonding slurry was used to bond the metallic spheres at points of contact. After drying, the cast foam was once again heat treated in hydrogen to reduce the bond slurry and sinter the structure. Several large pieces, approximately 15 x 10 x 2 cm, were fabricated using this process. Metallographic examination of the foam panels fabricated in this manner showed significantly less sphere wall porosity than magnetite processed samples. A cross section of a sphere wall fabricated in this manner is

depicted in Figure 3. The point contact bonds proved to be an exception, however. Figure 4 shows the porosity retained at the point contacts due to the reduction of the bond slurry. Additionally, the point contacts show cracking and complete separation. Again the expansion during the reduction process of Fe_2O_3 becomes problematic, and the substitution of Fe_3O_4 for Fe_2O_3 in the bond slurry was used as a solution.

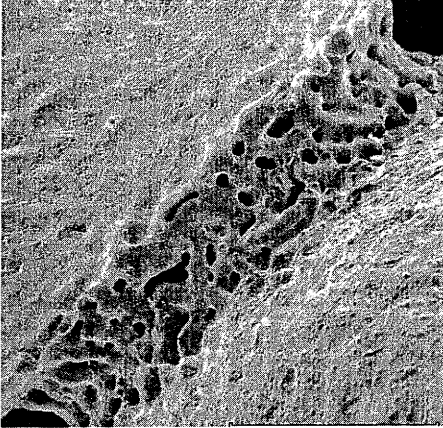


Fig. 3: Cross-section of Fe-Cr sphere wall showing complete densification. (100x)

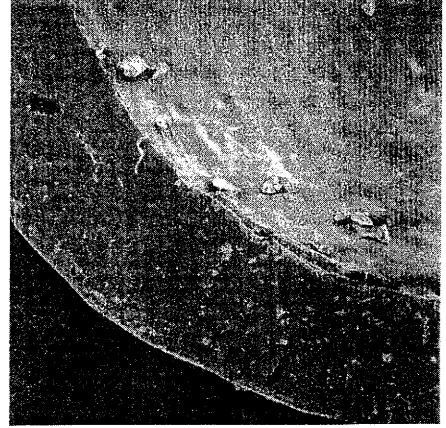


Fig. 4: Neck between two spheres showing significant porosity after reduction. (110x)

The formulation of the bond slurry was changed to accommodate magnetite and used to bond loose metallic spheres into a foam. The foam was hydrogen fired accordingly to obtain a fully reduced, densified metallic hollow sphere foam. Figures 5 and 6 show the sintered spheres and necks resulting from the use of the magnetite bond slurry.

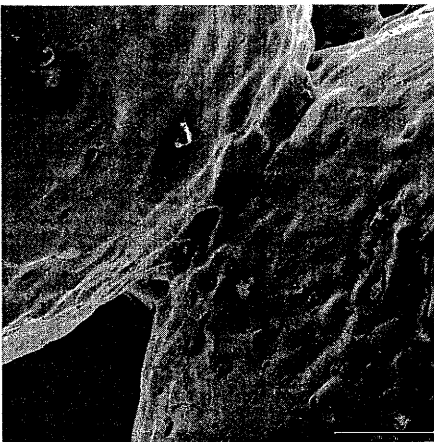


Fig. 5: Fe-Cr spheres bonded with magnetite slurry and reduced. (20x)

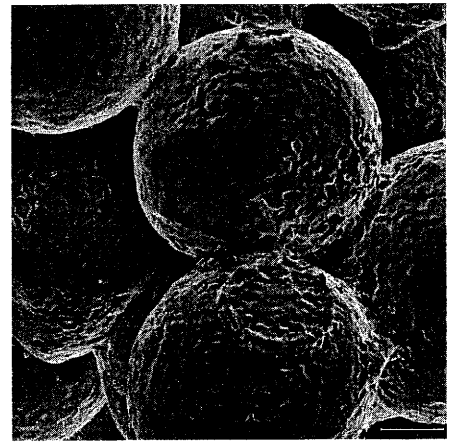


Fig. 6: Neck between two spheres bonded magnetite slurry and reduced. (50x)

2.4 Carburization and Heat Treatment

With the successful fabrication of a bulk foam, it is necessary to add carbon and heat treat the material to obtain optimal stainless steel properties. The composition Fe-12Cr is the basis for a martensitic stainless steel with a maximum of 0.15 wt.% carbon. Carburizing the foams required heating the samples to the austenizing temperature and allowing diffusion of carbon from surface into the bulk.^{8,9} Carbon was deposited on the surface using two different methods.

The first method used a polyfurfuryl alcohol-acetone solution in which the samples were dipped and dried. The polyfurfuryl alcohol deposited on the surface decomposes on heating to the austenizing temperature, leaving carbon on the surface. This method is not a conventional process and required no special equipment. Control of carbon contents, however, would have to be experimentally determined. The second method was the more conventional gas carburizing process, where CO and CO₂ are used to deposit carbon on the surface of the samples at the austenizing temperature. With the copious amounts of data available on this subject, a ratio of partial pressures of CO to CO₂ to obtain a particular carbon content was determined. Gas carburizing was the primary means by which the foam samples were carburized.

After carburizing, the cooling of the samples was controlled to obtain the desired microstructure. Samples were both furnace cooled and water quenched. A pearlitic microstructure was obtained from the furnace cool while martensite was obtained from the quench. The quenched samples were sub-zero quenched to convert any retained austenite to martensite and finally tempered at 400 °C for 2 hours. Samples were then mechanically tested.

3 Mechanical Properties

Various loose-sphere processed foam samples were deformed under uniaxial compression using a servo-hydraulic testing machine. Typical specimen size was 2 x 2 x 2.5 cm and typical strains were 60-80 percent. Figures 7 and 8 show the compression behavior of loose sphere processed foams, non-carburized and carburized, bonded with Fe₂O₃ slurry.

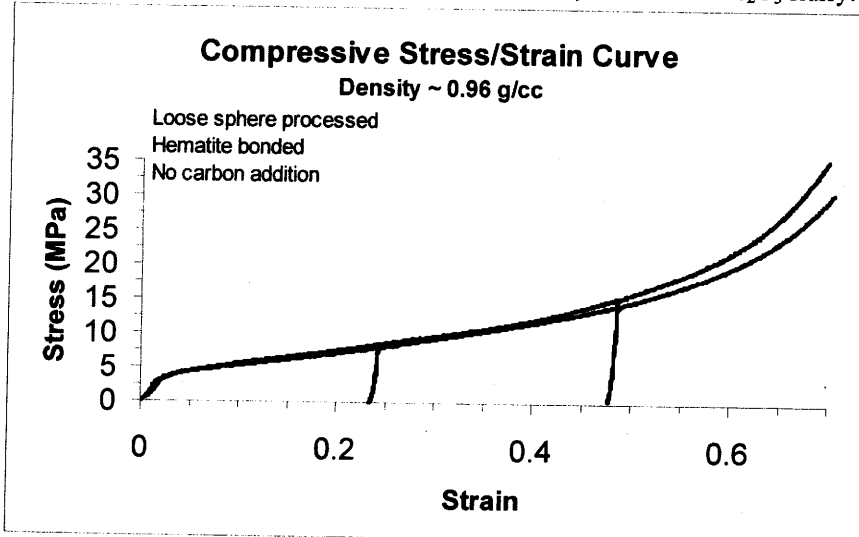


Fig. 7: Compressive data of loose sphere processed 88Fe-12Cr foam.

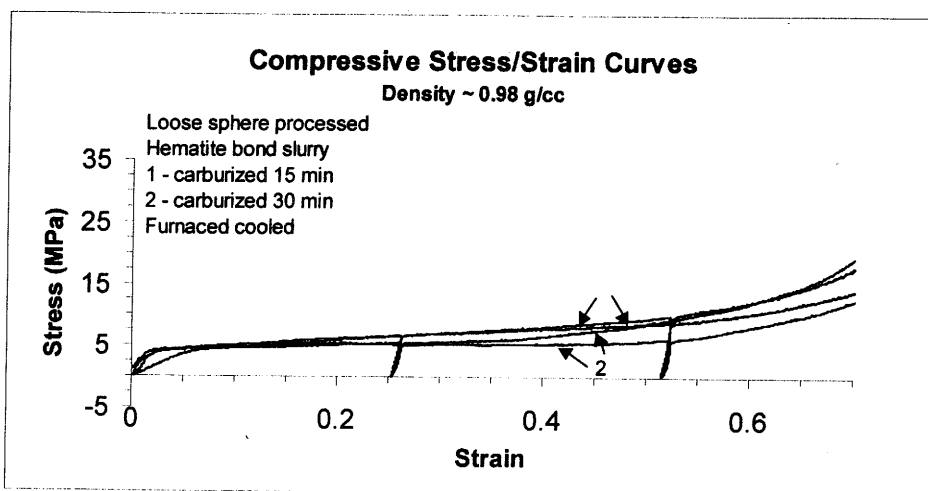


Fig. 8: Compressive data of loose sphere processed, carburized 88Fe-12Cr foam.

The yield strength of non-carburized samples approached 4 MPa, while carburized samples showed more than 4 MPa. Additionally, the carburized samples showed brittle behavior with respect to the non-carburized samples as seen by the shape of the stress/strain curve and the lower energy absorption of the carburized samples. Based on bulk properties of steel compared to Fe-Cr alloy alone, the carburized samples were expected to show much better results. The reason for the apparent discrepancy is assumed to lie in the porous bond phase as well as the carburization and heat treatment. The carburized samples were prepared using gas carburization with a $p\text{CO}/p\text{CO}_2$ ratio of 1.15:1. This is expected to yield a carbon content of 0.1 wt.% and is within the 0.15 wt.% maximum for 413 stainless steel. After carburizing, the samples were furnace cooled to allow formation of pearlite. It is believed that the samples oxidized sufficiently to embrittle the porous bond phase. The embrittled necks could not transfer the load and the outer spheres crumbled off the specimen as the load increased. Consequently, the effective cross-sectional area of the test specimens decreased as outer spheres fell off. Testing of individual spheres from these foams was also performed to further explore the problem. The individual carburized spheres also performed in a brittle manner, unable to attain strengths greater than the non-carburized spheres. While the combination of oxidation and porous bond phase is the most plausible explanation, confirmation needs to be made with measurements of carbon and oxygen contents.

Figure 9 shows the stress-strain behavior of foams bonded with the Fe_3O_4 slurry. The behavior is similar to that of the Fe_2O_3 bonded foam in Figure 7. Both foams show the characteristic ductile foam response. Taking into account density differences, the magnetite bonded foam did show a slight increase in yield strength, however. This is associated with better reduction and sintering of the bond phase. It is believed that, with better control of oxidation and carburization, the magnetite bonded foams will yield significantly better results than those achieved thus far.

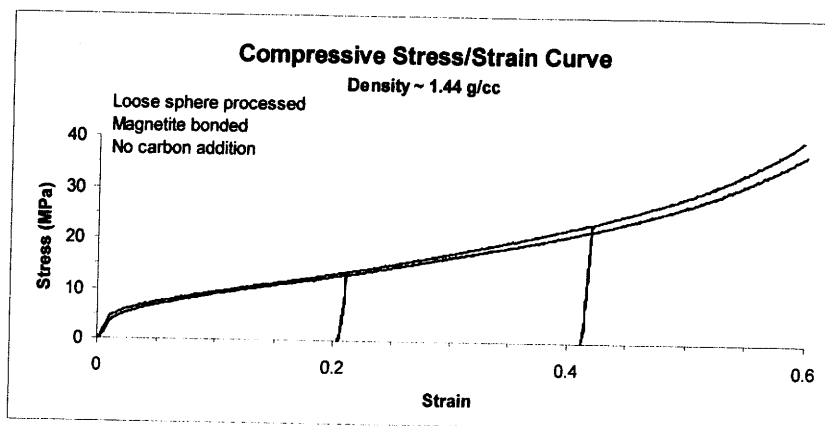


Fig. 9: Compressive data of magnetite bonded loose spheres.

4 Summary

The effort to scale up production of stainless steel hollow sphere foams has identified several areas in processing that will require continued diligence. The need to ensure the integrity of the foam structure is vital. Severe expansion during the reduction process leads to destruction of the foam before reduction has occurred, while weak neck bonds lead to early failure as the bonds, unable to transfer the forces adequately, break and causes the foam to crumble. The loose sphere processing and magnetite bond slurry have provided solutions to the problems encountered thus far. With the appropriate carburizing and heat treatment conditions, further progress will be made.

References

- [1] K. M. Hurysz, J. L. Clark, A. R. Nagel, C. U. Hardwicke, K. J. Lee, J. K. Cochran, and T. H. Sanders, Jr. "Steel and Titanium Hollow Sphere Foams," in Porous and Cellular Materials for Structural Applications, MRS Proceedings vol. 521, edited by D. Schwartz, *et al.*, (MRS, Pittsburgh, PA, 1998), pp 191-203.
- [2] A. R. Nagel, Closed Cell Steel Foams from Oxide Reduction, Masters Thesis, Georgia Institute of Technology, Oct. 1997.
- [3] Stephenson, ed., Direct Reduced Iron: technology and economics of production and use, Iron & Steel Society of AIME, Warrendale, PA, 1980.
- [4] L. Gibson and M. Ashby, Cellular Solids Structures and Properties, Pergamon Press, Elmsford, NY, 1988.
- [5] L. S. Darken and R. W. Gurry. "The system Iron-Oxygen. II. Equilibrium and Thermodynamics of Liquid Oxide and Other Phases." *J. Am. Chem. Soc.*, 1946, v. 68, pp. 798-816.
- [6] G. Krauss, Steels: Heat Treatment and Processing Principles, ASM International, Materials Park, OH, 1995.
- [7] Muan, Arnulf and Osborn, Phase Equilibria Among Oxides in Steelmaking, Addison Wesley Publishing Company, Reading, MA, 1965.
- [8] Carburizing and Carbonitriding, ASM Committee on Gas Carburizing, Metals Park, OH, 1977.
- [9] Stainless Steel, ASM International, 1994.